Tumor Cells Resistant to a Microtubule-Depolymerizing Hemiasterlin Analogue, HTI-286, Have Mutations in α- or β-Tubulin and Increased Microtubule Stability

Marianne S. Poruchynsky,*,‡ Jong-Hyeok Kim,‡,§ Eva Nogales,|| Tami Annable,⊥ Frank Loganzo,⊥ Lee M. Greenberger,⊥ Dan L. Sackett,# and Tito Fojo‡

Cancer Therapeutics Branch, The NCI Center for Cancer Research, National Cancer Institute, Bethesda, Maryland 20892, Molecular and Cell Biology Department, Howard Hughes Medical Institute, University of California, Berkeley, California 94720, Oncology Research, Wyeth Research, Pearl River, New York 10965, and National Institute of Child Health and Development, National Institutes of Health, Bethesda, Maryland 20892

Received April 7, 2004; Revised Manuscript Received August 16, 2004

ABSTRACT: Hemiasterlins are sponge-derived tripeptides that inhibit cell growth by depolymerizing existing microtubules and inhibiting microtubule assembly. Since hemiasterlins are poor substrates for P-glycoprotein, they are attractive candidates for cancer therapy and have been undergoing clinical trials. The basis of resistance to a synthetic analogue of hemiasterlin, HTI-286 (HTI), was examined in cell populations derived from ovarian carcinoma (A2780/1A9) cells selected in HTI-286. 1A9-HTI-resistant cells (1A9-HTI^R series) were 57−89-fold resistant to HTI. Cross-resistance (3−186-fold) was observed to other tubulin depolymerizing drugs, with collateral sensitivity (2−14-fold) to tubulin polymerizing agents. Evaluation of the percentage of polymerized and soluble tubulin in 1A9 parental and 1A9-HTI^R cells corroborated the HTI cytotoxicity data. At 22 °C or 37 °C, in the absence of any drug, the percentage of polymerized microtubules for each of the 1A9-HTI^R populations was greater than that in the 1A9 parental cells, consistent with more stable microtubules. Furthermore, microtubules in the 1A9-HTI^R populations were also more resistant to depolymerization at 4 °C and had more acetylated and detyrosinated (Glu-tubulin) α-tubulin, all characteristic of more stable microtubules. The 1A9-HTI^R cell populations exhibited either a single nucleotide change in the M40 β-tubulin isotype, S172A, or in two cell populations where no β-tubulin mutation was detected, mutations in the Kα-1 α-tubulin isotype, S165P and R221H in one resistant cell population and I384V in another. Unlike reports of mutations resulting in reduced drug affinity, the experimental data and location of mutations are consistent with resistance to HTI-286 mediated by microtubule-stabilizing mutations in β- or α-tubulin.

A structural cell component crucial for diverse cellular functions and survival, the dynamic microtubule network, along with its αβ-tubulin dimeric constituents, remains a well-recognized target in the search for more effective chemotherapeutic agents (*1*, *2*). Although a variety of antimicrotubule agents, such as the taxanes and vinca alkaloids, are widely used in the chemotherapy of cancer (*3*), their efficacy is limited by the presence of drug resistance mechanisms. One mechanism of resistance, drug efflux mediated by the transporter P-glycoprotein (MDR1; ABCB1),[1] confers resistance to the taxanes and vinca alkaloids (*4*). Recent efforts to discover tubulin targeted compounds that circumvent P-glycoprotein have identified the epothilones (*5*, *6*) and discodermolide (*7*), which, like taxanes (*8*, *9*), promote tubulin polymerization (*7*), and the hemiasterlins, which destabilize microtubules (MTs) (*10*−*13*).

The hemiasterlins are a group of cytotoxic tripeptides originally isolated from marine sponges (*11*, *13*, *14*) for which many analogues have been synthesized (*10*). HTI-286 (Figure 1) is a synthetic hemiasterlin (*15*) and, like other family members, hinders tubulin polymerization and induces dissolution of MTs (*12*, *13*) by binding to tubulin dimer (*16*) causing mitotic arrest and inhibition of cell proliferation (*10*, *12*, *15*). Radiolabeled photoaffinity analogues of HTI-286 have been shown to label the α-tubulin subunit (*17*). HTI-286 inhibits the growth of human tumor xenografts resistant to paclitaxel and vincristine due to the expression of MDR1 (*15*). HTI-286 is also active in tumor cell lines overexpressing the ABCG2 or MRP1 drug transporters (*15*). Our previous studies have determined that HTI-286 is active against cell lines selected for paclitaxel or epothilone resistance and harboring point mutations in β-tubulin at the taxane binding site.[2] The ability of HTI-286 to bypass diverse mechanisms

* Corresponding author. Telephone: (301) 496-6611. Fax: (301) 402-1608. E-mail: mporuch@helix.nih.gov.

‡ National Cancer Institute.

§ Present address: University of Ulasan, Asan Medical Center, Department of Obstetrics & Gynecology, Seoul, Korea.

|| University of California.

⊥ Wyeth Research.

National Institutes of Health.

[1] Abbreviations: HTI, HTI-286 (*N*,β,β-trimethyl-L-phenylalanyl-*N*^{1}-[(1*S*,2*E*)-3-carboxy-1-isopropylbut-2-enyl]-*N*^{1},3-dimethyl-L-valinamide, also known as SPA110); PTX, paclitaxel; 1A9-HTI^R, 1A9-HTI-resistant; Glu-tubulin, detyrosinated glu terminated tubulin; MDR1, ABCB1, P-glycoprotein; MTs, microtubules; ABCG2, ATP binding cassette transporter subfamily G member 2; MRP1, ABCC1, multidrug resistance protein; SRB, sulforhodamine B; TNE buffer, 50 mM Tris, pH 7.5, 100 mM NaCl, 2 mM EDTA, 1% NP-40, and protease inhibitors; CHO, Chinese hamster ovary.

10.1021/bi049300+ CCC: $27.50
Published on Web 10/15/2004

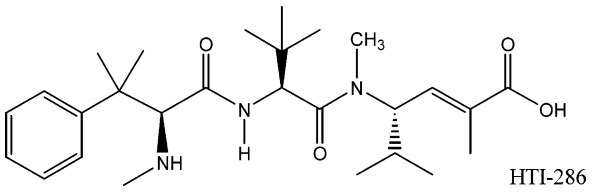

FIGURE 1: The chemical structure of the synthetic hemiasterlin tripeptide HTI-286.

of resistance distinguishes it from most tubulin targeted drugs presently used clinically.

To further understand the mechanisms of resistance to HTI-286, we have characterized 1A9 ovarian carcinoma cells subjected to chronic HTI-286 exposure. These resistant cells (1A9-HTI^R) displayed enhanced sensitivity to taxanes and other tubulin polymerizing drugs, were cross-resistant to vinca alkaloids and other hemiasterlins, lacked MDR1, and contained mutations in either α- or β-tubulin. The mutations were located outside the taxane-binding site (*18*) and appeared to confer stability to the microtubules of the 1A9-HTI^R cells. We found that, compared to the 1A9 parental cells, microtubules in each of the 1A9-HTI^R cell populations we isolated were resistant to the destabilizing effects of drugs or cold temperature, had a greater proportion of polymerized to soluble tubulin, and increased acetylated and detyrosinated α-tubulin, posttranslational modifications consistent with more stable microtubules (*19*−*22*).

MATERIALS AND METHODS

Compounds. Compounds were obtained either from Wyeth Research Laboratories (Pearl River, NY) [HTI-286 (Figure 1) (*N*,*β*,*β*-trimethyl-L-phenylalanyl-*N*^{1}-[(1*S*,2*E*)-3-carboxy-1-isopropylbut-2-enyl]-*N*^{1},3-dimethyl-L-valinamide, also known as SPA110) (*10*, *15*) and hemiasterlin analogues]; from NIH internal sources [sarcodyctin A, epothilone A, discodermolide, paclitaxel, vincristine, vinblastine, vinorelbine, docetaxel, eleutherobin, adriamycin, cryptophycin-1, dolastatin-10, maytansine, rhizoxin, colchicine, and colcemid]; or from CalbioChem (San Diego, CA) [phomopsin A].

Selection of HTI-286 Resistant Cells. A subclone of the A2780 human ovarian carcinoma cell line, 1A9, was maintained in RPMI medium supplemented with 10% fetal bovine serum, glutamine, 10 units/mL penicillin and 10 μg/mL streptomycin (*23*). 1A9 cells were selected as separate populations by initial exposure either to 1.0, 2.0, 2.5, or 4 nM HTI-286 as follows, and a total of nine populations exhibiting three mutation phenotypes were found: 1.0 nM, 1A9-HTI-βS172A(S1,S2,S5, and S6) and 1A9-HTI-αS165P;R221H; 2.0 nM, 1A9-HTI-αI384V; 2.5 nM, 1A9-HTI-βS172A(S3 and S4); or 4.0 nM, 1A9-HTI-βS172A(S7). After initial cytotoxicity assays and sequencing of tubulin, four HTI-286 resistant cell populations representative of the mutations observed (Table 1) were established by chronic exposure to 0.5−1.0 nM incremental concentrations of HTI-286 over several months. Thus 1A9-HTI-αI384V (maintained in 8 nM HTI-286) and 1A9-HTI-βS172A(S1), 1A9-HTI-βS172A(S3), and 1A9-HTI-αS165P;R221H cells (the latter three each maintained in 13 nM HTI-286) were those further characterized. When experiments were performed using

Table 1: Tubulin Mutations in 1A9 Cells Resistant to HTI-286

cell line populations[a]	β-tubulin M-40 isotype	α-tubulin K-α-1 isotype	β- or α-tubulin codon change	relative resistance to HTI-286
1A9 (parental)	WT	WT		1
1A9-HTI-βS172A(S1)[b]	172$^{Ser→Ala}$	WT	TCA → GCA	57
1A9-HTI-βS172A(S3)	172$^{Ser→Ala}$	WT	TCA → GCA	66
1A9-HTI-αI384V	WT	384$^{Ile→Val}$	ATT → GTT	65
1A9-HTI-αS165P;R221H	WT	165$^{Ser→Pro}$, 221$^{Arg→His}$	TCC → CCC CGC → CAC	89

[a] Parental 1A9 cell populations were separately selected for resistance to HTI-286. HTI-286 concentrations used in the initial selection were as follows: 1A9-HTI-βS172A(S1) and 1A9-HTI-αS165P;R221H, 1 nM; 1A9-HTI-βS172A(S3), 2.5 nM; 1A9-HTI-αI384V, 2.0 nM. The cells are maintained as described in Materials and Methods. [b] Five other HTI^R cell populations, 1A9-HTI-βS172A(S2 and S4−S7), each harboring the single 172$^{Ser→Ala}$ β-tubulin mutation, were also identified following the initial selection but not further advanced or characterized.

populations initially characterized or those maintained at higher drug concentrations, similar experimental results were always obtained. Therefore, results shown for all experiments, excluding the cytoxocity analyses for three other hemiasterlins, were performed using the cells maintained at the indicated concentrations of HTI-286. Prior to an experiment, all cells were grown in the absence of drug for 4−7 days.

Sequence Analysis of β- and α- Tubulin. RNA was prepared from the drug sensitive 1A9 parental and 1A9-HTI^R cells using the RNAStat reagent (Tel-Test, Inc., Friendswood, TX) according to the directions provided by the manufacturer. The GenBank accession numbers for the M40, K-α-1 and B-α-1 isotypes are J00314, NM 006082, and X01703, respectively. RT-PCR was performed by previously described methods (*23*). For PCR amplification and nucleotide sequencing of the M40 isotype of β-tubulin, six overlapping primer pairs were used as follows:

PCR primers

pair 1 $^{(-57)}$CTTGCCCCATACATACCTTGA$^{(-37)}$

$^{(765)}$GTTGACTGCCAACTTGCGGAG$^{(745)}$

pair 2 $^{(571)}$TTGGTAGAGAATACTGATGAG$^{(591)}$

GTAAGACGGCTAAGGGAACTG$^{(3'-UTR)}$

Sequencing primers

pair 3 $^{(19)}$ATCCAGGCTGGTCAATG$^{(35)}$

$^{(371)}$TCTGCCTCCTTCCGTACCAC$^{(352)}$

pair 4 $^{(280)}$TCTGGGGCAGGTAACAACT$^{(298)}$

$^{(645)}$CCTCAGAGTGCGGAAGCAGAT$^{(625)}$

pair 5 $^{(679)}$CTTGTCTCAGGCACCATGGAGT$^{(700)}$

$^{(1035)}$GGGGATCCATTCCACAAAGT$^{(1016)}$

pair 6 $^{(982)}$CAGATGCTTAACGTGCAGAACAAG$^{(1005)}$

$^{(1264)}$GATACTCAGAGACGAGGTCG$^{(1245)}$

PCR-amplified cDNA was purified with PCR Select-III spin columns and directly sequenced with the *Taq* DyeDeoxy

[2] Poruchynsky, M. S., and Loganzo, F. Unpublished observations.

terminator cycle sequencing kit following the manufacturer's instructions (Applied Biosystems, Inc.). The reaction products were purified with Centri-Sep spin purification columns, electrophoresed on 48-cm/4.75% polyacrylamide/urea gels, and analyzed by an automated DNA sequencing system (model 377; Applied Biosystems, Inc.).

For PCR amplification and nucleotide sequencing of the K-α-1 isotype of α-tubulin, five overlapping primer pairs were used as follows:

PCR primers

pair 1 $^{(-67)}$TGTCGGGGACGGTAACCGGG$^{(-48)}$

$^{(726)}$CAGGGAAGCAGTGATGGAGGA$^{(706)}$

pair 2 $^{(652)}$GATATCGAGCGCCCAACCTAC$^{(672)}$

AATTCTGGGAGCATGACATGC$^{(3'-UTR)}$

Sequencing primers

pair 3 $^{(269)}$AGCAGCTCATCACAGGCAAG$^{(288)}$

$^{(396)}$AAGACGGGTGCACTGGTCAG$^{(377)}$

pair 4 $^{(376)}$CTGACCAGTGCACCCGTCTT$^{(395)}$

$^{(615)}$GTCTACCATGAAGGCACAATC$^{(595)}$

pair 5 $^{(895)}$GCCAACCAGATGGTGAAATG$^{(914)}$

$^{(1020)}$CGTGCGCTTGGTTTTGATGG$^{(1001)}$

For PCR amplification and nucleotide sequencing of the B-α-1 isotype of α-tubulin, four overlapping primer pairs were used as follows:

PCR primers

pair 1 $^{(1)}$ATGCGTGAGTGCATCTCCATC$^{(21)}$

$^{(702)}$ACAATTTGACCTATTAACCTA$^{(682)}$

pair 2 $^{(659)}$CGTCCAACCTATACTAACCTG$^{(679)}$

CTTCCCTGTAAAAGCAGCACC$^{(3'-UTR)}$

Sequencing primers

pair 3 $^{(268)}$AGCAACTCATCACAGGCAAA$^{(287)}$

$^{(394)}$GAGACGCGTGCACTGGTCGG$^{(375)}$

pair 4 $^{(893)}$GCCAACCAGATGGTGAAATG$^{(912)}$

$^{(1018)}$GGTACGCTTGGTCTTGATGG$^{(999)}$

For K-α-1 or B-α-1, the reaction products were purified with Centri-Sep spin purification columns and analyzed by an automated DNA sequencing system (model 3100; Applied Biosystems, Inc.).

Cytotoxicity Assays and Growth Analysis of HTI-286 Resistant Cells. Cell survival was determined by the SRB method using cells that were grown in drug-free media for 4−7 days prior to plating in 96-well dishes (*23*). Cells were exposed to serial dilutions of each drug for 4 days prior to fixation, SRB staining, and IC_{50} determinations, calculated as described previously (*23*).

For growth analysis, cells were plated identically in six-well dishes in the absence of drug (−) or in the presence (+) of the HTI-286 concentration at which they are normally maintained (e.g. 8 or 13 nM, as described earlier). Cells were harvested and counted on the day of plating and on each of six consecutive days. The average doubling time for each cell line was calculated in hours by determining the average factor by which the cells increased in number over several days during their exponential phase of growth.

Tubulin Polymerization Assays. Cells were plated in 24-well dishes, grown to 60−80% confluency, and treated with either no drug or varying concentrations of drugs alone or sequentially at 37 °C. Cells were treated with drug for 5.5 h for the paclitaxel (PTX) dose response experiment, and in sequential drug experiments, the first drug incubations were for 2 h followed by the second incubation of 2.5 h. After the media was removed, cells were rinsed in 1X PBS at 22 °C, harvested at the same temperature in lysis buffer containing 0.1 M Pipes, 1 mM EGTA, 1 mM $MgSO_4$, 30% glycerol, 5% DMSO, 5 mM GTP, 0.125% NP-40, and protease inhibitors (Roche Diagnostics GmbH, Mannheim, Germany), including aprotinin [200 units/ml], pH 6.9 (*24*), and then centrifuged at ∼15000*g* at 22 °C for 30 min in an Eppendorf model 5402 temperature controlled centrifuge (Brinkmann Inst., Westbury, NY), to separate polymerized (P) from soluble (S) tubulin. Pellets of polymerized "P" tubulin were resuspended in a volume of lysis buffer equal to the soluble "S" fraction, each had gel sample buffer added (*23*), and equal aliquots separated by 7.5% SDS/PAGE. After transfer to Immobilon-P (Millipore Corp., Bedford, MA), immunoblotting was performed with anti α-tubulin [DMIA, Sigma, St. Louis, MO], followed by an HRP-conjugated secondary antibody (Amersham Biosciences UK Limited, U.K.) as previously described (*23*) and visualized using SuperSignal Reagents (Pierce Biotechnology, Rockford, IL).

Analysis of Tubulin Polymerization at Varying Temperatures and Centrifugation Conditions. Cells growing in drug free media were lysed for 20 or 30 min at 37 °C or 4 °C, respectively, in the buffer described above. To separate polymerized (P) from soluble (S) tubulin, samples were centrifuged at 186000*g* for 90 min using a TLA 55 rotor in a Beckman Optima Max ultracentrifuge, at the same temperature at which they were lysed. Identical samples lysed at 37 °C were also centrifuged at ∼15000*g* for 30 min in an Eppendorf model 5415C centrifuge (Brinkmann Inst., Westbury, NY) to compare this lower "*g*" force centrifugation with that performed at higher speed for longer time. Immunoblots were probed with anti α-tubulin (DM1A) as described above.

Comparison of Acetylated, Detyrosinated, and Total α-Tubulin in HTI Sensitive and Resistant Cells. Cell lysates were prepared by harvesting cells at 4 °C in TNE buffer (50 mM Tris, pH 7.5, 100 mM NaCl, 2 mM EDTA, 1% NP-40, and protease inhibitors (*25*)), vigorously vortexing, incubating at 4 °C for 15 min, and sonicating in a bath sonifier (Branson Sonifier 450) for 20−30 s to completely disrupt the cells. Total protein concentration in these clear lysates was measured using the Bio-Rad protein assay reagent (Bio-Rad Labs., Hercules, CA). Aliquots containing 35 μg of total protein were removed, and SDS was added to a final concentration of 0.5%, followed by vigorous vortexing before addition of gel sample buffer and the separation of proteins

by SDS−PAGE on four identically loaded gels. The proteins were transferred to Immobilon-P and probed with either α-tubulin antibody (DM1A), actin (Sigma, St. Louis, MO), acetylated α-tubulin (Clone 6-11B-1, Sigma, St. Louis, MO), or Glu-tubulin (detyrosinated α-tubulin). Antibody to detyrosinated tubulin was either obtained from Chemicon International (Temecula CA) or raised in rabbits using peptides that correspond to the detyrosinated carboxyl terminus of α-tubulin, according to published procedures (*26*), and was the kind gift of Dr. April Robbins, (NIDDK, NIH). Species appropriate HRP-conjugated secondary antibodies along with SuperSignal reagents were utilized to visualize the proteins as described above. Band intensities were quantified by densitometry using IPLabgel software.

Location of the Altered Amino Acid Residues in the αβ-Tubulin Dimer. The refined electron crystallography structure of the αβ-tubulin dimer (*27*) was used to localize the position of the mutated residues. These locations were also visualized in the context of a microtubule lattice (*28*, *29*). Visualization was carried out using the Program O (*30*), and Figures 7 and 8 were generated using PyMOL (PyMOL.SOURCE.NET).

RESULTS

Mutations in β- or α-Tubulin in 1A9 Cells Selected for Resistance to HTI-286. To further understand the mechanism of resistance to the hemiasterlins, a malignant cell culture experimental model was used. Ovarian carcinoma 1A9 cells were initially selected as nine separate resistant populations by exposure to either 1.0, 2.0, or 2.5 nM HTI-286, as indicated in Materials and Methods and Table 1, and then four were established by chronic increased exposure to HTI-286. The relative HTI-286 resistance of each of these populations compared to the 1A9 parental is shown in the right-hand column of Table 1 and ranges from 57- to 89-fold. As described, only 1A9-HTI-βS172A(S1), 1A9-HTI-βS172A(S3), 1A9-HTI-αI384V, and 1A9-HTI-αS165P;R221H cells, populations representative of all the mutations we observed (Table 1), were advanced to higher HTI-286 concentrations and further characterized.

Previous studies had shown that M40 was the predominant β-isotype (*23*), while K-α-1 and B-α-1 were the most abundant α-isotypes (*31*). Compared to the 1A9 parental cell line, the 1A9-HTI-βS172A(S1−S7) cell line populations each had a single heterozygous mutation in the M40 β-tubulin isotype, converting amino acid 172 from Ser to Ala [TCA → GCA]. No mutations were found in the K-α-1 and B-α-1 α-tubulin isotype. By comparison, 1A9-HTI-αI384V had a heterozygous mutation in the K-α-1 α-tubulin isotype, converting amino acid 384 from Ile to Val [ATT → GTT], while 1A9-HTI-αS165P;R221H had two homozygous mutations in K-α-1 converting amino acids 165 from Ser to Pro [TCC → CCC] and 221 from Arg to His [CGC → CAC]. No mutations were found in the B-α-1 α-tubulin isotype in each of these cell line populations. We feel it likely that the βS172A mutation was a preexisting clone in the 1A9 parental cell population, present in a small percentage of cells, and that under HTI-286 selection, offspring of this clone gave rise to the seven 1A9-HTI-βS172A(S1−S7) populations. This mutation would be undetectable in the 1A9 parental unselected cell population and is thus corroborated by our sequencing data where only wild type sequences are noted

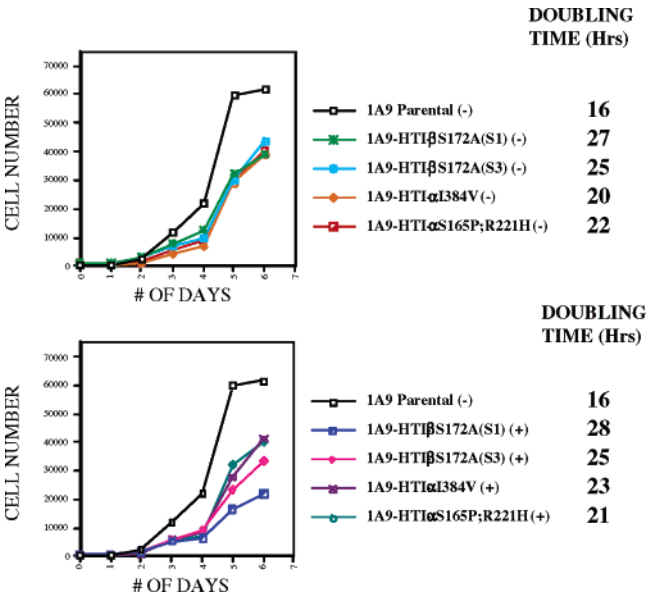

FIGURE 2: Representative doubling times (hours) and growth curves spanning a six day period for the 1A9 parental cells and the HTI-286 resistant cells grown either in the absence (−) or in the presence (+) of HTI-286 as follows: 1A9-HTI-βS172A(S1) [13 nM]; 1A9-HTI-βS172A(S3) [13 nM]; 1A9-HTI-αI384V [8 nM]; and 1A9-HTI-αS165P;R221H [13 nM].

(Table 1). It is probable that, under the selective pressure of HTI-286, the cells were able to expand in number, which is more likely than the mutation occurring seven times at the same position. However, we cannot absolutely exclude that this represents a "hot-spot" where this mutation was acquired seven separate times.

When the growth characteristics of exponentially growing 1A9 parental and HTI^R cell populations were assessed, the average doubling times determined for the cells ranged from 16 to 28 h. Representative growth curves for the cells are displayed in Figure 2. The differences between the doubling times for HTI^R cells with or without HTI-286 were not significant (Figure 2). The 1A9-HTI^R cells do not require the presence of HTI-286 in the medium for viability.

Furthermore, RT-PCR failed to detect expression of MDR1 in any of the cell lines (data not shown), consistent with previous data showing that HTI-286 has negligible or weak interactions with P-glycoprotein (*15*).

Resistance Profile of 1A9 Cells Selected with HTI-286. We next characterized the cross-resistance profile of the HTI^R cell populations. To simplify the cytotoxicity evaluation, cross-resistance values for three resistant populations representing each mutation profile identified are shown in Table 2. As shown, the cells were also 2−9-fold cross-resistant to other hemiasterlins, and the evaluation for these drugs was performed prior to advancing the populations in higher concentrations of HTI-286. Furthermore, the cells were 3−186-fold cross-resistant to other MT depolymerizing agents including podophyllotoxin, and four drugs that bind to the vinca domain of tubulin (*32*), vinorelbine, vincristine, vinblastine, and rhizoxin, as well as dolastatin-10 and cryptophycin-1, which bind to the vinca-peptide domain (*33*). The cells were also marginally resistant (2−3-fold) to colchicine, colcemid, and maytansine, but not to phomopsin A, the latter drug interacting with the vinca-peptide domain. In contrast, the cells were 2−14-fold more sensitive to MT

Table 2: Resistance Profile of 1A9 Cells Selected with HTI-286

compound	IC_{50} (nM) 1A9 parental	fold resistance[a] 1A9-HTI-βS172A-(S1)	1A9-HTI-αI384V	1A9-HTI-αS165P;-R221H
hemiasterlins				
HTI-286 (SPA110)	0.3 ± 0.03[b]	52	65	89
SPA115	12.6	7	3	9
hemiasterlin	0.2	9	7	6
hemiasterlin A	0.5	3	3	2
other vinca-peptide domain				
dolastatin-10	0.036 ± 0.0007	10	7	10
cryptophycin-1	0.009 ± 0.0001	4	4	7
phomopsin A	1270	1		1
vinca domain				
vinorelbine	0.2 ± 0.008	78	122	186
vincristine	0.6	20	27	13
vinblastine	0.6	10	11	10
rhizoxin	34.7 ± 1.6	7	3	4
maytansine	0.141 ± 0.003	2	3	3
colchicine site				
podophyllotoxin	34.8 ± 0.01	4	3	3
colchicine	6.1 ± 5.7	2	2	2
colcemid	11.1 ± 0.05	3	1	3
polymerizing agents				
paclitaxel	0.45 ± 0.01	0.12	0.15	0.32
docetaxel	3.0 ± 0.2	0.15	0.18	0.22
discodermolide	10.4 ± 0.5	0.22	0.11	0.30
epothilone A	2.2 ± 0.01	0.13	0.13	0.24
sarcodyctin A	185 ± 21	0.08	0.07	0.41
eleutherobin	51 ± 0.7	0.09	0.09	0.20
DNA active agent				
adriamycin	6.0 ± 0.6	0.56	~0.17	0.74

[a] The fold resistance is the relative resistance compared to parental cells. [b] Values shown are mean (nM) ± standard deviation. Where multiple cytotoxicity assays were performed (2−10 repeats), standard errors are shown.

polymerizing drugs including paclitaxel, docetaxel, discodermolide, epothilone A, sarcodyctin A, and eleutherobin. The resistant cells were also as sensitive to adriamycin (1−5-fold), a drug that utilizes DNA as its intracellular target. Taken together, these cytotoxicity profiles suggested that the mutations identified in either β- or α-tubulin were altering the stability of microtubules rather than interfering with hemiasterlin binding, thereby conferring resistance to tubulin targeting depolymerizing drugs.

Tubulin Polymerization in 1A9-HTI-286 Resistant Cells in Response to Paclitaxel. To test whether the tubulin in the resistant cells was more stable than that of the 1A9 parental cell line and to evaluate the response of tubulin from these cells to a MT stabilizing drug, experiments separating polymerized "P" from soluble "S" tubulin were performed at 22 °C. For the studies that assessed tubulin polymerization and depolymerization properties and those that described the posttranslational modifications on α-tubulin, the 1A9-HTI-βS172A(S1), 1A9-HTI-βS172A(S3), 1A9-HTI-αI384V, and 1A9-HTI-αS165P;R221H cell populations were used.

As can be seen in Figure 3, in the absence of drug there was a much greater proportion of tubulin in the "P" compared to the "S" fraction, in all of the resistant cells with the tubulin mutations (P:S ratios approximately 50:50) (see % P values, Figure 3) as compared with the 1A9 parental cells (P:S ratio approximately 14:86) (Figure 3). This strongly indicated the presence of more stable microtubules in resistant cells. Furthermore, when cells were treated with increasing concentrations of PTX, the tubulin shift to the "P" fraction was noted over the 5−30 nM PTX range and incremented the baseline "P" fraction in each of the 1A9-HTI^R resistant cell populations (Figure 3). Thus the increased sensitivity of the 1A9-HTI^R cells to PTX in the cytotoxicity experiments likely reflects the already increased "P" fraction baseline.

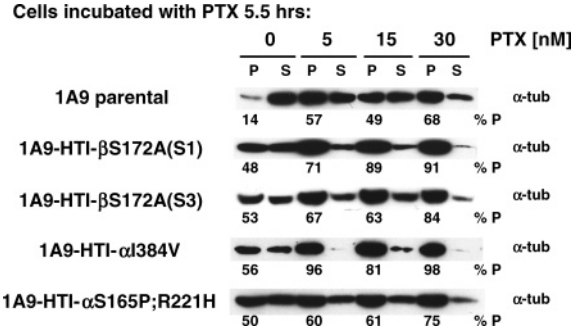

FIGURE 3: Comparison of tubulin polymerization between 1A9 parental cells and 1A9-HTI-286 resistant cells in response to paclitaxel (PTX). Cells were treated at 37 °C for 5.5 h either with no drug (0) or with 5, 15, or 30 nM paclitaxel (PTX) and solubilized in lysis buffer at 22 °C. Lysates were centrifuged at ~15000*g* at 22 °C for 30 min to separate polymerized (P) from soluble (S) tubulin and the proportion in each fraction evaluated by western blot using antibody to total α-tubulin (see Materials and Methods for details). The percent of polymerized tubulin (% P) was calculated by multiplying the fraction of tubulin in the polymerized fraction [P/(P + S)] by 100 for each "P−S" pair.

The lysis buffer we utilize to retrieve the polymerized and soluble tubulin fractions is used at 22 °C, and without the addition of paclitaxel, to optimize effects of mutations or of drugs added to cells, not to assess the steady-state polymer level inside cells at 37 °C. The conditions allow the comparison of tubulin distribution between the polymerized "P" and soluble "S" fractions under a specific set of conditions, for HTI-sensitive and resistant cells. Although the assay to determine the % of tubulin in the "P" versus "S" fraction has variation from day to day, over the course of many experiments using a variety of conditions of drug incubation, we consistently observed the distinct trends of differences between the 1A9-HTI^R cell populations and 1A9 parental cells for each individual experiment. Thus, every experiment has its control. For example, the greater amount of the % of tubulin in the "P" fraction for each of the 1A9-HTI^R cell populations was routinely observed when compared to that of the 1A9 parental cells, despite a large standard deviation (e.g. 1A9 parental % P = 14.5 ± 9.6; 1A9-HTI-βS172A(S1) % P = 30.2 ± 13.6; 1A9-HTI-βS172A(S3) % P = 52 ± 1.0; 1A9-HTI-αI384V % P = 34.4 ± 16.1; and 1A9-HTI-αS165P;R221H % P = 41.3 ± 13.9). Experimental results shown in each figure for a particular experiment are representative.

Depolymerization of Microtubules by HTI-286 in Resistant or Sensitive Cells Pretreated with Paclitaxel. To further explore the characteristics of the resistant cell populations with tubulin mutations, the study shown in Figure 4 was carried out to establish if HTI-286 could reverse the polymerizing effect of paclitaxel. The effect of HTI-286 on the depolymerization of microtubules was determined by pretreating cells with PTX followed by incubation with both drugs simultaneously. Densitometry of bands visualized on the films provided approximate values for partition of tubulin between "P", polymerized, and "S", soluble, fractions. As

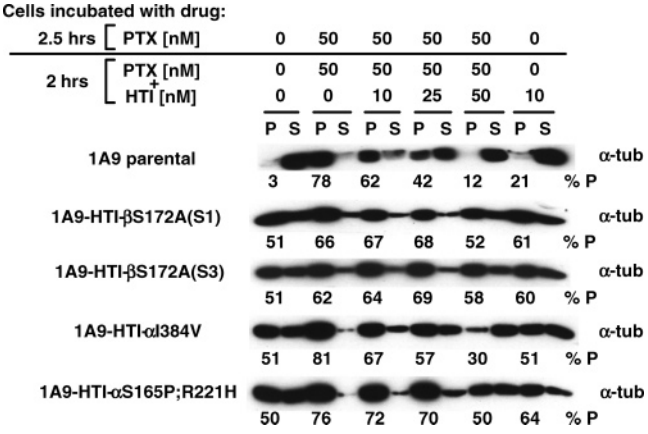

FIGURE 4: Comparison of the depolymerization of microtubules by HTI-286 in 1A9 parental or 1A9-HTI-286 resistant cells pretreated with paclitaxel. Cells were treated with either 50 nM paclitaxel or no drug (0), for 2.5 h at 37 °C. The medium was removed and cells previously exposed to PTX were reexposed to PTX with or without 0−50 nM HTI-286 for an additional 2 h at 37 °C. Cells in additional wells were incubated solely in 10 nM HTI-286 for the latter 2 h at 37 °C. All cells were lysed at 22 °C, and the lysates were centrifuged at ~15000*g* at 22 °C for 30 min to separate polymerized (P) from soluble (S) tubulin and evaluated by western blot using antibody to total α-tubulin. The percent of polymerized tubulin (% P) was calculated by multiplying the fraction of tubulin in the polymerized fraction [P/(P + S)] by 100 for each "P−S" pair.

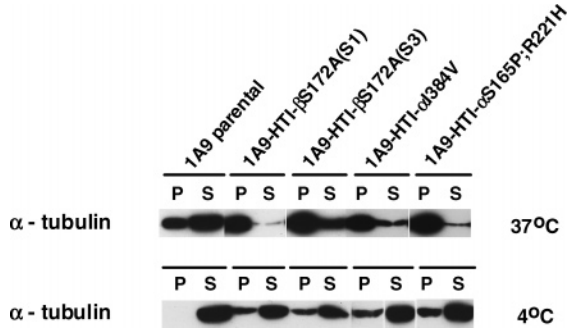

FIGURE 5: Analysis of tubulin polymerization at 37 °C and microtubule cold stability in 1A9 parental cells and 1A9-HTI-286 resistant cells. Cells growing in drug free media were incubated either for 20 min at 37 °C or for 30 min at 4 °C in lysis buffer. Samples were centrifuged to separate polymerized (P) from soluble (S) tubulin at 186000*g* for 90 min at either 37 °C or 4 °C, respectively. Western blots of samples were probed with antibody to α-tubulin.

previously shown in Figure 3, when harvested at 22 °C in the absence of drug (first column "P−S" pair), there was proportionally more tubulin in the "P" fraction in the resistant cell populations as compared with the 1A9 parental cells. Furthermore, as shown in Figure 4 in the second pair of "P−S" lanes, the high concentrations of PTX used (50 nM) induced comparable levels of polymerization in parental and resistant cell populations despite the hypersensitivity of the resistant cells to PTX (compare to 30 nM as highest concentration in Figure 3). However, consistent with the relative resistance to HTI-286 following PTX treatment, HTI-286 was unable to depolymerize MTs in the resistant cells to the extent it depolymerized parental cell microtubules (especially compare 25 and 50 nM HTI lanes). The response to the HTI + PTX combination also correlated with the relative resistance to HTI-286, e.g. in the 1A9-HTI-αI384V cells that were less resistant to HTI the % P after 50 nM HTI-286 was 30% compared to 50−58 % P for the resistant cells with the other tubulin mutations. The difficulty in depolymerizing microtubules in the resistant cells is consistent with the interpretation that these cells have more stable microtubules as a result of their tubulin mutations, and that these microtubules can be stabilized to a greater extent by paclitaxel and other MT-stabilizing agents. Furthermore, in the absence of other drugs, the MTs of the HTI^R cell populations are more resistant to depolymerization by HTI-286. For each of the HTI^R cell populations with tubulin mutations, higher concentrations (50 nM) were required to completely depolymerize the tubulin and shift it entirely from the "P" to the "S" fraction compared to the 1A9 parental cells where lower concentrations were adequate (data not shown).

Analysis of Microtubule Cold Stability in HTI-286 Sensitive and Resistant 1A9 Cells. In the absence of drug, we demonstrated in the preceding experiments (Figures 3 and 4) an increased proportion of polymerized "P" tubulin compared to soluble "S" tubulin, for each of the resistant cell populations compared to the 1A9 parental cells when they were harvested, lysed, and centrifuged at 22 °C. We wanted to determine whether harvesting cell lysates incubated at the higher temperature of 37 °C as well as centrifuging at higher "*g*" (gravitational) forces would result in a further increase in the proportion of tubulin retrieved in the "P" compared to the "S" fraction. As shown in Figure 5, where samples were centrifuged at 180000*g* versus 15000*g* in previous figures, qualitatively, we observed more tubulin in all of the "P" fractions compared to "S" fractions for each of the resistant cells, and even a slight increment in "P" fraction for the 1A9 parental cells after incubating the lysate at 37 °C for 20 min (compare the 37 °C results with those in Figures 3 and 4). This was true even when the lysates were centrifuged at the lower force of 15000*g*, for 30 min (data not shown), but was more dramatic for each cell line when the identically treated samples were centrifuged at the greater force of 186000*g*, for 90 min at 37 °C, as shown.

Furthermore, to evaluate the microtubule destabilizing effects of cold temperature on the various mutant tubulins, cell lysates were incubated at 4 °C for 30 min prior to a high speed 186000*g*, 90 min centrifugation, at 4 °C. The microtubules of the resistant cell populations were more stable to the depolymerizing effect of cold temperature than those of the 1A9 parental cells, since a shift of the tubulin to the "S" fraction from the "P" fraction at 4 °C was apparent but incomplete for the resistant cells (Figure 5). No polymerized tubulin was retrieved in the "P" fraction of the 1A9 parental cells, despite the lengthy and high "*g*" force centrifugation. These results are consistent with increased microtubule stability in the resistant cells harboring the tubulin mutations.

Comparison of Acetylated, Detyrosinated, and Total α-Tubulin in HTI Sensitive and Resistant Cells. Our assays that quantitated the distribution between polymerized and soluble fractions of tubulin in the resistant cells under a variety of conditions indicated that stabilized microtubules, less susceptible to cold- and drug-induced depolymerization, were present in the resistant cells. It is well established that tubulin can be altered by posttranslational modifications, and several of these occur exclusively on α-tubulin (*19*, *20*). Although

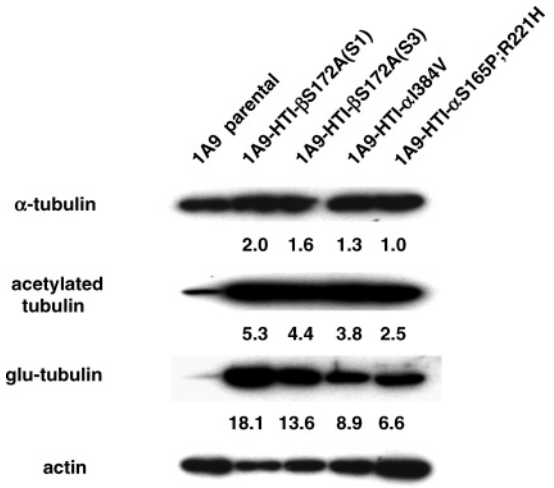

FIGURE 6: Comparison of acetylated, detyrosinated, and total α-tubulin in 1A9 parental cells or 1A9-HTI-286 resistant cells. Cells harvested in TNE buffer, pH 7.5, were sonicated to clarity, had SDS added to a final concentration of 0.5%, followed by addition of SDS-gel sample buffer. Aliquots containing 35 μg of total protein from complete cell lysates were separated by SDS−PAGE on four identically loaded gels. The western blots were probed either with antibody to total α-tubulin, acetylated α-tubulin, glu-tubulin (detyrosinated α-tubulin), or actin. The numbers below the bands represent the fold difference in amount of that protein relative to the amount in 1A9 parental cells, normalized to actin.

the precise relationship between these tubulin modifications and microtubule stability has not been elucidated, several of the changes were defined as markers of more stable microtubules (*21*, *22*). Acetylation and detyrosination are two such modifications (*21*, *22*), the latter resulting in the exposure of the penultimate amino acid on α-tubulin, a glutamic acid. As shown in Figure 6, we assessed the levels of expression of total α-tubulin, as well as these two modified α-tubulin forms, in whole cell lysates of the resistant and parental cells. The values below the bands represent the fold difference in the expression quantitated in each cell line relative to 1A9 parental cells after normalization to actin. We observed a marked increase of both acetylated (2.5−5.3-fold) and Glu-tubulin (detyrosinated) α-tubulin (6.6−18.1-fold) consistent with more stable microtubules. Finally, in additional studies we observed similar levels of stathmin (*34*) protein expression in the postnuclear lysates of the 1A9 parental and resistant cells (data not shown).

Mutation Mapping and Structural Hypothesis of Resistance. Figure 7 displays the location of the single residue in β-tubulin and the three residues in α-tubulin that were mutated in the hemiasterlin resistant cell lines. The potential impact on microtubule stability and resistance to HTI-286 by mutations at these sites in the heterodimers is addressed in detail in the Discussion. Details of the longitudinal relationship between neighboring αβ-tubulin heterodimers at the interdimer interface are shown in Figure 8.

DISCUSSION

The microtubule cytoskeleton is well recognized as a chemotherapeutic target, and there is an ongoing search for microtubule targeting agents (MTAs) with increased efficacy (*3*, *35*). Drug resistance to MTAs in cultured malignant cells has been attributed to diverse mechanisms, including drug

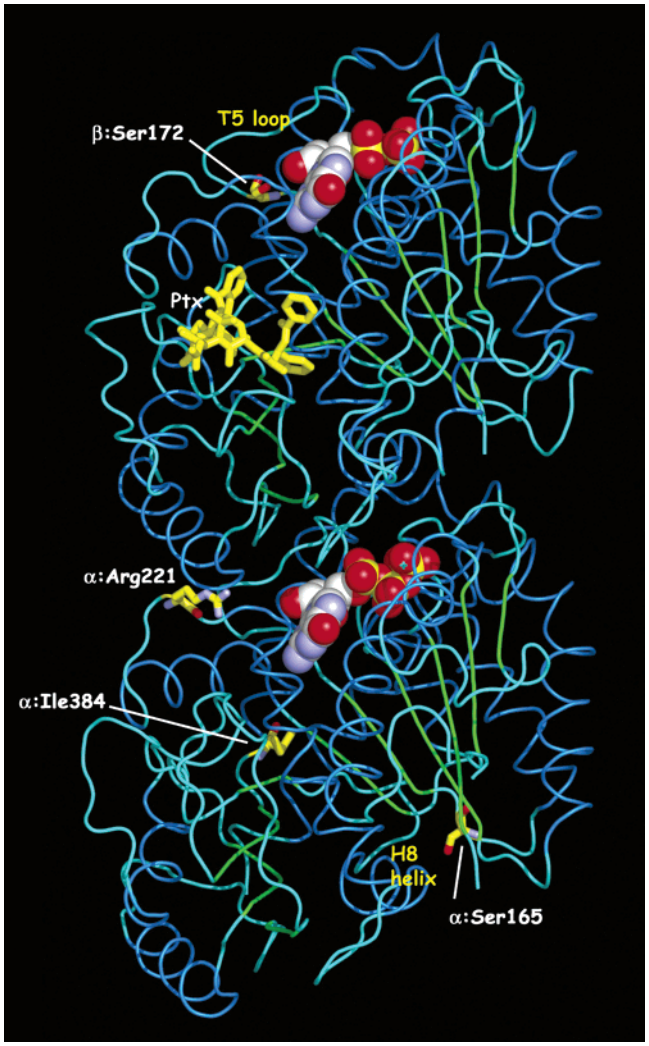

FIGURE 7: Location of the residues mutated in the αβ-tubulin heterodimer in 1A9 cells resistant to HTI-286. The positions of the single altered residue in β-tubulin and the three residues altered in α-tubulin are indicated (molecular tube structures). Loop T5 and helix H8 are shown. The exchangeable and nonexchangeable GTP sites are indicated on β- and α-tubulin, respectively (spherical model structures). For reference, a molecule of paclitaxel is indicated in its β-tubulin binding site.

efflux transporters (*4*), altered tubulin isotype expression (*36*−*39*), and tubulin mutations (*5*, *6*, *23*, *36*−*43*), the latter resulting in either altered drug binding or putative changes in microtubule stability. The hemiasterlins, a group of naturally occurring tripeptides that potently inhibit cell proliferation and depolymerize microtubules, have been recently described (*10*−*14*) and are currently undergoing clinical testing in humans. Antimitotic/cytotoxic and structural−activity relationship data has been described for a large series of synthetic hemiasterlin analogues, including HTI-286 (*10*). In the present report we describe several hemiasterlin resistant human cell line populations with mutations in either α- or β-tubulin. The evidence indicates that these mutations confer significant levels of resistance to HTI-286 by stabilizing microtubules, a mechanism similarly described in Chinese hamster ovary (CHO) cells (*43*, *44*).

We have taken advantage of an assay conceived by Cabral et al. (*44*), to separate polymerized "P" from "S" soluble tubulin fractions by centrifugation. This procedure, and subsequent modifications of it, have been widely utilized and

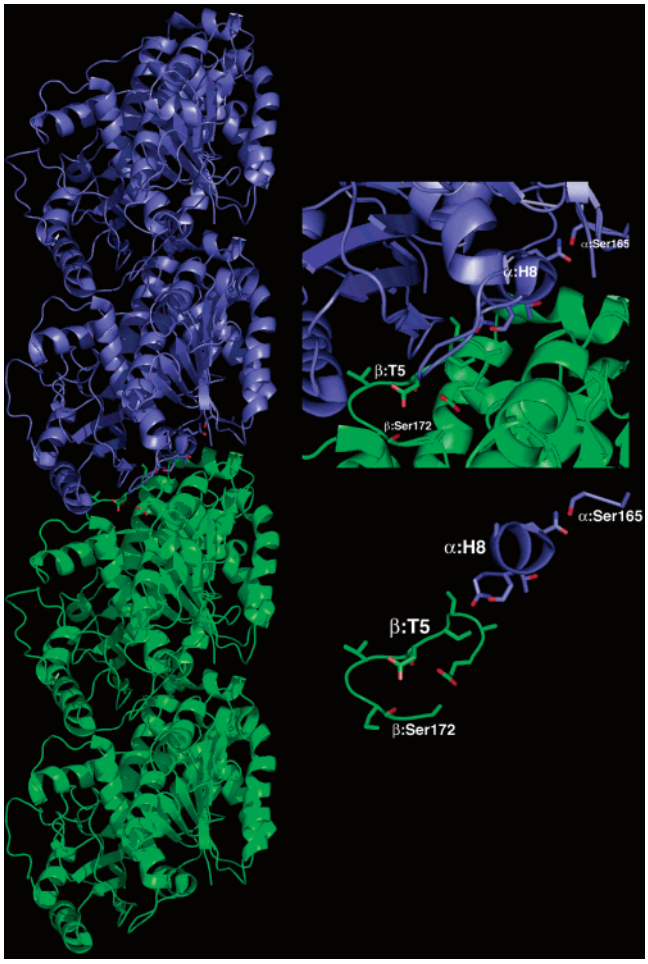

FIGURE 8: Interdimer interface between neighboring α*β*-tubulin heterodimers. The longitudinal relationship between α-tubulin structures of one heterodimer (lavender) (αSer165, α-tubulin helix H8) and structures of *β*-tubulin on the next heterodimer (green) (*β*-tubulin loop T5 and *β*Ser172) is displayed.

allow a quick and rather consistent assessment of the percent of tubulin polymer in cells under a variety of experimental conditions. An increase in the "P" fraction serves as one indicator of stabilized tubulin. In the present study, we were able to demonstrate the presence of more stable microtubules in the resistant cell populations by several criteria. First, in the absence of drug, an increased proportion of tubulin was found in the polymerized compared to soluble tubulin fractions for the resistant cell populations, compared to the 1A9 parental cells. The percent of tubulin in the polymerized fraction was also greater in the resistant than the parental cells when lysates were incubated at 37 °C. Moreover, the microtubules of the resistant cells were more stable to the depolymerizing effect of cold temperature, since a shift of their tubulin to the soluble fraction at 4 °C was incomplete in contrast to the parental cell tubulin. We would note that a mutation in a *β*-tubulin isotype of yeast resulting in cold stable microtubules has been previously reported (*45*, *46*). Our assay of polymerized and soluble tubulin in cells treated with a sequential drug regimen also indicated that HTI-286 can substantially reverse tubulin polymerization induced by PTX in 1A9 parental cells, but not in the resistant populations. In addition, we were able to demonstrate posttranslational modifications on α- tubulin consistent with increased microtubule stability. Tubulin can undergo numerous post-translational modifications, including phosphorylation, polyglutamylation, polyglycylation, deglutamylation, acetylation, and tyrosination/detyrosination (*20*, *21*). Although the functions of the modifications on tubulin remain unclear (*47*), deglutamylation, acetylation, and detyrosination occur on α-tubulin and are at least indicative of stable microtubules (*20*−*22*). Acetylation occurs on lysine 40 near the amino terminus of α-tubulin (*48*) and does not appear to increase the levels of stable microtubules but instead accumulates on existing stable MTs (*21*, *22*). Glu-tubulin is formed when the last residue on α-tubulin, a tyrosine, is removed by tubulin-carboxypeptidase and the glutamic acid is exposed (*19*−*22*). This detyrosination only occurs on α-tubulin in polymerized microtubules (*20*, *47*) and restoration of the tyrosine residue to α-tubulin is via tyrosine-ligase and occurs exclusively on soluble α*β*-tubulin heterodimers (*20*). We observed a marked increase of both acetylated and detyrosinated α-tubulin in the resistant cells, indicating the presence of more stable microtubules. Unlike the tubulin detyrosination described as a frequent occurrence in aggressive breast cancers with poor prognosis (*49*) that is apparently a result of suppression of tubulin tyrosine-ligase (*50*), the increase here is a result of the existence of more stable microtubules secondary to either *β*- or α-tubulin mutations. Further studies on the significance of the presence of these and other tubulin modifications (*51*) in clinical samples will be of interest.

While HTI-286 selected resistant cell populations were also found to be resistant to other members of the hemiasterlin family, their cytotoxicity profile indicated cross-resistance to other vinca-peptide or vinca binding site agents, with collateral sensitivity to tubulin polymerizing agents. Although there is evidence that hemiasterlins associate or overlap with the vinca binding domains on tubulin (*33*) and the cytotoxicity profile could be explained in part by alterations in the binding site, the pattern was consistent with the presence of more stable microtubules in the cells as a mechanism of resistance, exemplified by the higher baseline amount of polymerized tubulin. One group has elegantly demonstrated that epothilone B, like taxanes, alters MT dynamics at low concentrations (*52*), and this may be the case for hemiasterlins as well. It would be of interest to characterize the MT dynamics in this regard in the HTI-286 selected cells that exhibited more stable MTs, comparing both MT polymerizing and depolymerizing agents.

Tubulin sequences are some of the most conserved known, likely due to the requirement of maintaining polymerization interfaces. Moreover, the fine-tuning of how these interfaces are regulated to achieve dynamic instability adds further complexity and necessitates sequence optimization that leaves little room for viable residue changes. Thus, to ensure continued cell survival, mutations that will overcome drug effect must still maintain the ability for tubulin self-assembly and assembly regulation. Efficient antimitotic ligands should bind to available sites on the surface of the tubulin subunit and alter the self-assembly properties of the protein. Resistance to ligands that bind at sites not directly involved in polymerization can be mediated by mutations without detriment, since these sites are more likely to tolerate mutations without an effect on normal tubulin assembly. This may be the case for PTX, where a significant number of mutations resulting in resistance are localized at the known drug binding site, ascribing diminished PTX binding affinity.

If, on the other hand, the antimitotic agent uses a site that requires tight sequence conservation, e.g. those with a more general target since the binding site will be broadly conserved across species, one would predict that mutations causing resistance that do not eliminate tubulin polymerization entirely should be localized away from the drug binding site and have effects other than inhibition of drug binding. These should be mutations that alter MT dynamics in the opposite direction of the drug's effect. Thus, one would expect stabilizing mutations for depolymerizing agents and destabilizing mutations for polymerization-promoting drugs, so as to counter the drug's effect. The mutations we describe in this work apparently increase the stability of the MTs, conferring general resistance to depolymerizing agents and sensitivity to stabilizing ones, and are thus an example of this type of resistance mechanism.

We identified four different mutations in tubulin in the 1A9 cells selected for resistance to HTI-286. One mutation occurred in β-tubulin, whereas the other three were located in α-tubulin. On the basis of recent structural models (*18*, *27*, *53*), the positions of the mutant residues were determined in the three-dimensional tubulin structure (Figure 7). Serine β172 was located in the T5 loop, which in β-tubulin is involved in ribose binding at the exchangeable GTP site (Figure 7) and in longitudinal contacts between tubulin dimers (Figure 8). A mutation at this residue could affect this polymerization interface making it more stable. A resistance to destabilizing drugs and sensitivity to polymerizing ones would be predicted, and this is consistent with our observations. A Pro to Ala mutation at β173 was recently found in HeLa cells resistant to epothilone B (*5*), and altered microtubule stablility was hypothesized in that report as well.

As for the amino acids mutated in α-tubulin, Ser 165 makes an intramolecular hydrogen bond with Gln 256 in helix H8 (Figure 8). This helix in α-tubulin is a central part of the longitudinal interface between dimers (*18*, *27*). Furthermore, it contains Glu 254, a residue required for hydrolysis of the GTP in β-tubulin upon polymerization (*53*). We would speculate that the serine to proline mutation could result in a mislocalization of helix H8 resulting in a decreased hydrolysis rate, the final result being the overall stabilization of the microtubule cytoskeleton. It is also interesting to note that Ser 172 in β-tubulin and Ser 165 in α-tubulin are connected through a network of interactions centered around helix H8 in α-tubulin at the polymerization interface (*18*, *27*). A second α-tubulin mutation in the cells with the Ser 165 mutation involved Arg 221, a residue that is far from a polymerization interface but is exposed near the intradimer interface (*27*). It is located near helices H6 and H7 in α-tubulin and interacts longitudinally with residues in H10 on β-tubulin (*27*, see Table 2). A change here could influence the interaction between the β- and α-tubulin monomers and alter microtubule stability. Finally, we identified a mutation involving Ile 384 in α-tubulin. This residue is buried in a hydrophobic pocket, and mutation to a smaller side chain as we observed (Ile → Val) could result in a change in the stability of the monomer. β172 and α165 are not conserved positions in the tubulin sequence, while α384 is a valine residue in plants and algae. In contrast, α221, an arginine, is totally conserved in known tubulin sequences. Notably, R221H appeared as a double mutation together with S165P, as it is likely that it would have been a nonviable mutation on its own.

Thus, we believe that the mutations we observed in the resistant cells would likely exert effects on microtubule stability, rather than on the interaction between HTI-286 and tubulin. We would note that although a preliminary report using two photoaffinity analogues of HTI-286 labels the C-terminal region of α-tubulin, none of the residues mutated in our resistant cells are located in the region of α-tubulin implicated in HTI-286 binding (*17*). Other groups have identified mutations in α- or β-tubulin, and have inferred consequences on microtubule stability in human tumor cell lines selected with tubulin polymerizing agents (*5*, *6*, *42*). In addition, one report of CHO cells that were UV-irradiated and then selected with the tubulin depolymerizing agents colcemid or vinblastine (*43*) also identified a variety of mutations in α- or β-tubulin and implicated the 2-fold resistance they observed with putative altered microtubule stability. In earlier work, the same group reported tubulin mutations in CHO cells affecting MT stability (*54*) and in transfected CHO cells, a decrease in acetylated MTs, consistent with decreased MT stability (*55*).

Stathmin, a cytosolic protein that associates with tubulin dimers and MTs and functions to enhance depolymerization (*34*), was expressed similarly in the 1A9 parental and resistant cells (data not shown). Moreover, none of the mutations we identified occurred in the putative stathmin binding region of α-tubulin, helix 10 (*34*). Thus, although convincing evidence has been presented in other models (*5*, *37*), we believe it unlikely that stathmin plays a role in resistance in these cells.

Finally, we would mention briefly that, unlike our previous experience with paclitaxel and epothilone isolates where the wild type gene was silenced (*23*, *40*), in two of the three HTI-286 selections, the wild type gene continued to be expressed. While we are investigating this further, we believe this can be explained by the fact that in the paclitaxel and epothilone selections the mutations affected drug binding, while in the present situation microtubule stability was affected, and this can likely impact the polymer even if only 50% of the residues are mutant. For example a mutation affecting GTP hydrolysis might stabilize the microtubule even if present only on alternate dimers.

We conclude that the mutations identified in the 1A9 resistant cell populations selected with HTI-286 enhance microtubule stability and likely confer resistance to HTI-286 and other MT depolymerizing agents while simultaneously increasing susceptibility to MT polymerizing drugs. The difficulty in performing the selections, together with the occurrence of mutations only in regions of tubulin not associated with drug binding, as well as the absence of other resistance mechanisms, may all be viewed as favorable attributes for this class of drugs. One hopes this will translate into clinical benefit for patients with cancer.

REFERENCES

1. Downing, K. H. (2000) Structural basis for the interaction of tubulin with proteins and drugs that affect microtubule dynamics, *Annu. Rev. Cell Dev. Biol. 16*, 89−111.
2. Jordan, M. A., Wendell, K., Gardiner, S., Derry, W. B., Copp, H., and Wilson, L. (1996) Mitotic block induced in HeLa cells by low concentrations of paclitaxel (Taxol) results in abnormal

mitotic exit and apoptotic cell death, *Cancer Res. 56*, 816−825.
3. Rowinsky, E. K., Tolcher, A. W. (2001) Antimicrotubule agents, in *Cancer Principles and Practice* (J. Devita, V. T., Hellman, S., Rosenberg, S. A., Eds.) 6th ed., pp 431−452, Lippincott Williams and Wilkins, Philadelphia.
4. Gottesman, M. M., Fojo, T., and Bates, S. E. (2002) Multidrug resistance in cancer: role of ATP-dependent transporters, *Nat. Rev. Cancer 2* (1), 48−58.
5. He, L., Huang Yang, C.-P., and Horwitz, S. (2001) Mutations in β-tubulin map to domains involved in regulation of microtubule stability in epothilone-resistant cell lines, *Mol. Cancer Ther. 1*, 3−10.
6. Verrills, N. M., Flemming, C. L., Liu, M., Ivery, M. T., Cobon, G. S., Norris, M. D., Haber, M., and Kavallaris, M. (2003) Microtubule alterations and mutations induced by desoxyepothilone B: implications for drug-target interactions, *Chem. Biol. 10*, 597−607.
7. Stachel, S. J., Biswas, K., and Danishevsky, S. J. (2001) The epothilones, eleutherobins, and related types of molecules, *Curr. Pharm. Des. 7*, 1277−1290.
8. Horwitz, S. B. (1992) Mechanism of action of taxol, *Trends Pharmacol. Sci. 13*, 134−136.
9. Eisenhauer, E. A., and Vermorken, J. B. (1998) The taxoids. Comparative clinical pharmacology and therapeutic potential, *Drugs 55*, 5−30.
10. Nieman, J. A., Coleman, J. E., Wallace, D. J., Piers, E., Lim, L. Y., Roberge, M., and Andersen, R. J. (2003) Synthesis and Antimitotic/Cytotoxic activity of hemiasterlin analogues, *J. Nat. Prod. 66*, 183−199.
11. Talpir, R., Benayahu, Y., Kashman, Y., Pannell, L., and Schleyer, M. (1994) Hemiasterlin and geodiamolide TA: two new cytotoxic peptides from the marine sponge hemiasterella minor (kirkpatrick), *Tetrahedron Lett. 35*, 4453−4456.
12. Andersen, H. J., Coleman, J. E., Andersen, R. J., and Roberge, M. (1997) Cytotoxic peptides hemiasterlin, hemiasterlin A and hemiasterlin B induce mitotic arrest and abnormal spindle formation, *Cancer Chemother. Pharmacol. 39*, 223−226.
13. Gamble, W. R., Durso, N. A., Fuller, R. W., Westergaard, C. K., Johnson, T. R., Sackett, D. L., Hamel, E. Cardellina, J. H., II, and Boyd, M. R. (1999) Cytotoxic and tubulin-interactive hemiasterlins from Auletta sp. and Siphonochalina spp. Sponges, *Bioorg. Med. Chem. 7*, 1611−1615.
14. Coleman, J., De Silva, D., Kong, F., Andersen, R., and Allen, T. (1995) Cytotoxic peptides from marine sponge cymbastela sp., *Tetrahedron 51*, 10653−10662.
15. Loganzo, F., Discafani, C. M., Annable, T., Beyer, C., Musto, S., Hari, M., Tan, X., Hardy, C., Hernandez, R., Baxter, M., Singanallore, T., Khafizova, G., Poruchynsky, M. S., Fojo, T., Nieman, J. A., Ayral-Kaloustian, S., Zask, A., Andersen, R. J., and Greenberger, L. M. (2003) HTI-286, a synthetic analog of the tripeptide hemiasterlin, is a potent anti-microtubule agent that circumvents P-glycoprotein-mediated resistance in vitro and in vivo, *Cancer Res. 63*, 1838−1845.
16. Krishnamurthy, G., Cheng, W., Lo, M.-C., Aulabaugh, A., Raznikov, A., Ding, W., Loganzo, F., Zask, A., and Ellestad, G. (2003) Biophysical characterization of the interactions of HTI-286 with tubulin heterodimer and microtubules, *Biochemistry 42*, 13484−13495.
17. Nunes, M., Kaplan, J., Loganzo, F., Zask, A., Ayral-Kaloustian, S., and Greenberger, L. M. (2002) Two photoaffinity analogs of HTI-286, a synthetic analog of hemiasterlin, interact with alpha-tubulin, *Eur. J. Cancer. 38* (Suppl 7), S119.
18. Snyder, J. P., Nettles, J. H., Cornett, B., Downing, K. H., and Nogales, E. (2001) The binding conformation of Taxol in β-tubulin: a model based on electron crystallographic density, *Proc. Natl. Acad. Sci. U.S.A. 98*, 5312−5316.
19. Barra, H. S., Arce, C. A., and Argarana, C. E. (1988) Posttranslational tyrosination/detyrosination of tubulin, *Mol. Neurobiol. 2*, 133−153.
20. MacRae, T. H. (1997) Tubulin post-translational modifications—enzymes and their mechanisms of action, *Eur. J. Biochem. 224*, 265−278.
21. Infante, A. S., Stein, M., Zhai, Y., Borisy, G., and Gundersen, G. G. (2000) Detyrosinated (Glu) microtubules are stabilized by an ATP-sensitive plus-end cap, *J. Cell Sci. 113*, 3907−3919.
22. Palazzo, A., Ackerman, B., and Gundersen, G. G. (2003) Tubulin acetylation and cell motility, *Nature 241* (Jan 16), 230.
23. Giannakakou, P., Sackett, D. L., Kang, Y. K., Zhan, Z., Buters, J. T., Fojo, T., and Poruchynsky, M. S. (1997) Paclitaxel-resistant human ovarian cancer cells have mutant β-tubulins that exhibit impaired paclitaxel-driven polymerization, *J. Biol. Chem. 272*, 17118−17125.
24. Thrower, D., Jordan, M. A., and Wilson, L. (1991) Quantitation of cellular tubulin in microtubules and tubulin pools by a competitive ELISA, *J. Immunol. Methods 136*, 45−51.
25. Poruchynsky, M. S., Wang, E. E., Rudin, C. M., Blagosklonny, M. V., and Fojo, T. (1998) Bcl-x_L is phosphorylated in malignant cells following microtubule disruption, *Cancer Res. 58*, 3331−3338.
26. Gundersen, G. G., and Bulinski, J. C. (1984) Distinct populations of microtubules: tyrosinated and nontyrosinated α-tubulin are distributed differently in vivo, *Cell 38*, 779−789.
27. Lowe, J., Li, J., Downing, K. H., and Nogales, E. (2001) Refined Structure of αβ-Tubulin at 3.5 Å Resolution, *J. Mol. Biol. 313*, 1045−1057.
28. Nogales, E., Whittaker, M., Milligan, R. A., and Downing, K. H. (1999) High-Resolution Model of the Microtubule, *Cell 96*, 79−88.
29. Li, H., DeRosier, D. J., Nicholson, W. V., Nogales, E., and Downing, K. H. (2002) Microtubule Structure at 8 Å Resolution, *Structure 10*, 1317−1328.
30. Jones, E. Y., Walker, N. P., and Stuart, D. I. (1991) Methodology employed for the structure determination of tumour necrosis factor, a case of high non-crystallographic symmetry, *Acta Crystallogr. A 47*, 753−70.
31. Nicoletti, M. I., Valoti, G., Giannakakou, P., Zhan, Z., Kim, J. H., Lucchini, V., Landoni, F., Mayo, J. G., Giavazzi, R., and Fojo, T. (2001) Expression of β-tubulin isotypes in human ovarian carcinoma xenografts and in a sub-panel of human cancer cell lines from the NCI-anticancer drug screen: correlation with sensitivity to microtubule active agents, *Clin. Cancer Res. 7*, 2912−2922.
32. Rai, S. S., and Wolff, J. (1996) Localization of the vinblastine-binding site on β-tubulin, *J. Biol. Chem. 271*, 14707−14711.
33. Bai, R., Durso, N. A., Sackett, D. L., Hamel, E. (1999) Interactions of the sponge-derived antimitotic tripeptide hemiasterlin with tubulin: comparison with dolastatin 10 and cryptophycin 1, *Biochemistry 38*, 14302−14310.
34. Cassimeris, L. (2002) The oncoprotein 18/stathmin family of microtubule destabilizers, *Curr. Opin. Cell Biol. 14*, 18−24.
35. McDaid, H. M., Mani, S., Shen, H.-J., Muggia, F., Sonnischsen, D., and Horwitz, S. B. (2002) Validation of the pharmacodynamics of BMS-247550, an analogue of Epothilone B, during a phase I clinical study, *Clin. Cancer Res. 8* 2035−2043.
36. Orr, G. A., Verdier-Pinard, P., McDaid, H., and Horwitz, S. B. (2003) Mechanisms of Taxol resistance related to microtubules, *Oncogene 22*, 7280−7295.
37. Verdier-Pinard, P., Wang, F., Martello, L., Burd, B., Orr, G. A., and Horwitz, S. B. (2003) Analysis of tubulin isotypes and mutations from taxol-resistant cells by combined isoelectrofocusing and mass spectrometry, *Biochemistry 42*, 5349−5357.
38. Kavallaris, M., Tait, A. S., Walsh, B. J., He, L., Horwitz, S. B., Norris, M. D., and Haber, M. (2001) Multiple microtubule alterations are associated with vinca alkaloid resistance in human leukemia cells, *Cancer Res. 61*, 5803−5809.
39. Burkhart, C. A., Kavallaris, M., and Horwitz, S. B. (2001) Opinion. The role of β-tubulin isotypes in resistance to antimitotic drugs, *Biochim. Biophys. Acta 1471*, 01−09.
40. Giannakakou, P., Gussio, R., Nogales, E., Downing, K., H., Zaharevitz, D., Bollbuck, B., Poy, G., Sackett, D., Nicolaou, K. C., and Fojo, T. (2000) A common pharmacophore for epothilone and taxanes; molecular basis for drug resistance conferred by tubulin mutations in human cancer cells, *Proc. Natl. Acad. Sci. U.S.A. 97*, 2904−2909.
41. Poruchynsky, M. S., Annable, T., Kim, J., Fojo, T., Loganzo, F., and Greenberger, L. (2001) Tumor cells resistant to a tubulin-depolymerizing hemiasterlin analog, WAY-174286, display different resistance mechanisms, including mutations in α- or β-tubulin, *Clin. Cancer Res. 7* (Suppl.), 3810s.
42. Martello, L. A., Verdier-Pinard, P., Shen, H.-J., He, L., Torres, K., Orr, G. A., and Horwitz, S. B. (2003) Elevated levels of microtubule destabilizing factors in a taxol-resistant/dependent A549 cell line with an α-tubulin mutation, *Cancer Res. 63*, 1207−1213.

43. Hari, M., Wang, Y., Veeraraghavan, S., and Cabral, F. (2003) Mutations in α- and β-tubulin that stabilize microtubules and confer resistance to colcemid and vinblastine, *Mol. Cancer Ther. 2*, 597−605.
44. Minotti, A. M, Barlow, S. B., and Cabral, F. (1991) Resistance to antimitotic drugs in Chinese hamster ovary cells correlates with changes in the level of polymerized tubulin, *J. Biol. Chem. 266*, 3987−3994.
45. Gupta, M. L., Bode, C. J., Dougherty, C. A., Marquez, R. T., and Himes, R. H. (2001) Mutagenesis of β-tubulin cysteine residues in *Saccharomyces cerevisiae*: mutation of cysteine 354 results in cold-stable microtubules, *Cell Motil. Cytoskeleton 49*, 67−77.
46. Richards, K. L., Anders, K. R., Nogales, E., Schwartz, K., Downing, K. H., and Botstein, D. (2000) Structure-Function Relationships in Yeast Tubulins, *Mol. Biol. Cell. 11*, 1887−1903.
47. Gundersen, G. G. (2002) Evolutionary conservation of microtubule-capture mechanisms, *Nature 3*, 6−14.
48. L'Hernault, S. W., and Rosenbaum, J. L. (1985) *Chlamydomonas* α-tubulin is posttranslationally modified by acetylation on the ϵ-amino group of a lysine, *Biochemistry 24*, 473−478.
49. Miahle, A., Lafanechere, L., Treilleux, I., Peloux, N., Dumontet, C., Bremond, A., Panh, M.-H., Payan, R., Wehland, J., Margolis, R.-L., and Job, D. (2001) Tubulin Detyrosination Is a Frequent Occurrence in Breast Cancers of Poor Prognosis, *Cancer Res. 61*, 5024−5027.
50. Lafanechere, L., Courtay-Cahen, C., Kawakami, T., Jacrot, M., Rudiger, M., Wehland, J., Job, D., and Margolis, R. L. (1998) Suppression of tubulin tyrosine ligase during tumor growth, *J. Cell Sci. 111*, 171−181.
51. Lafanechere, L., and Job, D. (2000) The third tubulin pool, *Neurochem. Res. 25*, 11−18.
52. Kamath, K., and Jordan, M. A. (2003) Suppression of microtubule dynamics by Epothilone B is associated with mitotic arrest, *Cancer Res. 63*, 6026−6031.
53. Nogales, E. (2000) Structural insights into microtubule function, *Annu. Rev. Biochem. 69*, 277−302.
54. Boggs, B., and Cabral, F. (1987) Mutations affecting assembly and stability of tubulin: evidence for a nonessential beta-tubulin in CHO cells, *Mol. Cell. Biol. 7*, 2700−2707.
55. Gonzalez-Garay, M. L., Chang, L., Blade, K., Menick, D. R., and Cabral, F. (1999) A beta-tubulin leucine cluster involved in microtubule assembly and paclitaxel resistance, *J. Biol. Chem. 274*(34), 23875−23882.

BI049300+